Probing First Sources Using Global 21cm Signal on Constraining Primordial Black Hole

Subham Patra

Department of Physics, Presidency University, Kolkata-700073, West Bengal, India.

E-mail:subhampatra200@gmail.com

(Received: Jun 25, 2025, Revised: Jul 16, 2025, Accepted: Jul 26, 2025, Published: Sep 30, 2025)

Abstract: The red shifted 21-cm emission from neutral hydrogen is a promising tool to unveil the mysteries of the epoch of reionization and cosmic dawn. Ongoing and upcoming experiments such as the GMRT, LOFAR, MWA, SKA are aiming to detect the 21-cm signal statistically through quantities such as the power spectrum, bi-spectrum etc. Recent observations by the EDGES experiment suggest that the intergalactic medium may be much colder during the cosmic dawn than what we expect from the standard cosmological model. The power spectrum and bi-spectrum of the 21-cm signal from reionization and cosmic dawn are expected to different if the intergalactic medium is colder. In this project we wish to explore the impact of the colder intergalactic medium on the power spectrum and bispectrum.

Keywords: Cosmic Microwave background radiation (CMBR), red-shift, EDGES, primordial black hole (PBH).

I Introduction

The early universe was started through Big Bang. At that time the Universe was so dense and used to contain a high temperature and the redshift, z was very high. After a few intervals, inflation occurs then the "Quark glow phase" happened within a few seconds. After "Nucleosynthesis" the He (Helium) atoms formed as ionized form. Due to very high temperature, the electrons and protons randomly moved and scattering occurs with the photons. But for high-temperature electrons and protons could not combine with photons. After a few years, the temperature was decreased, and the energy of the photons decreased on which number of photons were decreased. Then the temperature of the universe gradually decreased with the adiabatic expansion of the Universe. Nearly at 3000k of the temperature and red shift, z =1000 photons were no longer capable to scatter with electrons and protons. At that phase, the Rayleigh radiation is originated called the "surface of flux scattering".

Finally, electrons and protons were collaborated with photons and get recombined. This phase is called the "Epoch of recombination [1–4]". After that the radiation-free electrons and protons have their ineffective scattering forms the "Neutral hydrogen (HI)" and the photons were moved freely in the Universe. The non-reacted photons still exist and they are caused by the Black Body radiation for high wavelength Rayleigh radiation. That in 1964 Robert Wilson and Aron Penzias suddenly discovered CMBR (Cosmological Background Radiation). The temperature of CMBR with a function of red-shift is 2.725k(1+z). After the formation of neutral hydrogen, there is no source of light. But in the early Universe stars are not formed. A star is the only source of visible light the Universe is dark. So, this age is called as Dark Age of the universe. The Dark Age occurred after the CMB and Recombination. After passing a very long period the universe got expanded at the red-shift - 25-30, stars and galaxies are formed, the sources of light are found. This turns the Dark Age into the light age and this period was named "Cosmic Dawn". The emitting of light of high energy photons produces the X-ray, γ-ray, etc. Which are highly ionized and the highly energized photons coming from the Universe did the separation of electrons and protons.

In the above context, we see that the Red Shift plays a great role in the history of the Universe. But in the present age of the Universe, the Red Shift is equal to zero. When we study the evolution of HI (Ionized Hydrogen) we came to know that in the Universe nearly 70% of dark energy, 26% of dark matter, and 4% baryons are present. The 4% of the baryons contain 75% of hydrogen and 25% of helium in the Universe. For the ancient Universe, according to the Hubble law, $v = Hd$ and $z = v/c$ the velocity of the ancient Universe is more due to more redshifts. For 75% of hydrogen in the Universe, the hydrogen cloud is gradually expanding. This may cause the early Universe hydrogen was going far away from us and the wavelength is becomes The term (1+z) is equal to the 1/scale factor(a(t)). So, now in the present-day universe, we want to detect the 21 cm signal such as Power spectrum, Bi spectrum, etc, by using some radio astronomical tools such as LOFAR, MWA, GMRT, PAPER, etc.

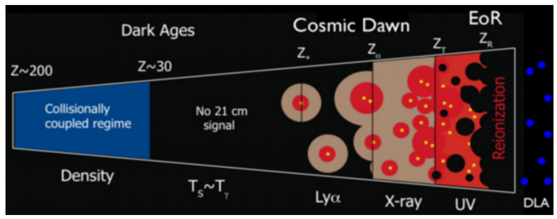

Figure 1: In the above diagram we measure the Cosmological Background temperature T_{CMB} or T_γ, Spin temperature T_s and the brightness temperature T_b due to radiative transfer by the help of telescopes and different astronomical tools.

Now, we mainly focus in the power spectrum and the optical depth, which is the only key terms that is very helpful to derive the followings equations. We also study the specific intensity and the rate of change of the specific intensity with the path dependent coordinate from there we get the general form of optical depth. The concept of differential brightness temperature is significantly helpful and here we do the further calculation of the differential brightness temperature and studied it analytically. We follow that the transition for the optical depth is significantly small at all incidental red shifts. In the expression of optical depth, we have the form of Hubble parameter there we study the cosmological parameters such as radiation density, matter density, curvature density and so on. The following graphs for optical depth and differential brightness temperature we take interval of red shift as 6 to 100 and the variation of spin temperature define that for low value of spin temperature the optical depth increase rapidly with the red shift and the differential brightness temperature is decrease rapidly i.e, the negative slope. Here we get the expression of dark matter power spectrum which is very much effective in the recent trends to detect excess radio background this is the most relevant concept in 21 cm physics and cosmology [5].

Now we introduce a great idea for finding the anomalous absorption rate of HI in the global 21 cm signal, i.e., the EDGES (Experiment to Detect the Global Epoch of Reionization Signature) signal of intensity $I_{21} \approx (1 - T_R/T_S)$ by the baryonic gas at red shifts in the range $z \approx 15 \rightarrow 21$,where T_R is the radiation temperature of the background and T_s is the spin temperature of the HI. If $T_R \gg T_S$, this implies the increase in absorption rate in the background radiation and if $T_R \ll T_S$, this imply the increase in emission rate in the background radiation. Here we study a new technique for cooling the hydrogen gas that depends mainly on baryon-dark matter interactions by the effects of dark energy. In an alternative way, we consider the injection of soft photons (in radio frequency and low energy) to increase consistently with the Cosmic Microwave Background (CMB) constraints [6,7]. We consider a toy model as Primordial black hole (PBH) [8] that has the same approach to analyze the energy injection due to a population of $O(1 \sim 100)M_\odot$ primordial black holes (PBHs), with constraining the possible PBH in DM abundance [9]. But we know that there has no radiation in the primordial black hole, so how to emit energy on to the PBHs? Under gravitational collapse, PBHs forms in the early universe and the surrounding gaseous material falls inside the black hole and this will convert into electromagnetic energy.

The whole process of the absorption rate of the 21 cm global signal is studied in analytical way and finally we get the spectral emissivity in terms of red shift and the fraction of primordial black hole f_{PBH} as unity, after that we find the energy absorption rate that can give a correct estimation of the absorption rate of HI in the global 21 cm signal. For finding the spectral emissivity we apply adopted formalism for injection of soft photons i.e., low-energy photons in the background and the gas accretion model [10,11] help to calculate total radiative intensity of the PBHs and then we describe the thermal and ionization history of the baryonic medium for finding the absorption rate of global 21cm signal. If we take the fraction of primordial black hole in terms of the kinetic temperature T_K and mass of the primordial black hole M_{PBH} then we get the fraction is less than unity and we find a contour plot $(f_{PBH} \times f_E)\ vs\ M_{PBH}$ from that we estimate the kinetic temperature T_K in the EDGES signal [12].

II 21cm Physics & Cosmology

II.a Origination of 21 cm line.

In the context we want to study the light which is originate in 21cm .So, now we may consider the ground state in the hydrogen spectra as n=1.

The spin of electrons and protons in the hydrogen atom have their sum of angular momentum is equal to total angular momentum (F) as,

$$\mathbf{F} = \mathbf{S} + \mathbf{I}, \tag{1}$$

where S is the spin of electrons and I is the spin of protons.

Electron, S=1/2	Proton, I=1/2
$\mathbf{S.S} = s(s+1)\hbar^2$ $S_z = m_s\hbar$ Where $m_s = \pm\frac{1}{2}$	$\boldsymbol{I.I} = I(I+1)\hbar^2$ $I_z = m_z\hbar$ Where $m_z = \pm\frac{1}{2}$

Figure 2: Properties of Electron-Proton spin.

So ,for the above condition, the Eigen value of F is,

$$\mathbf{F}.\mathbf{F} = F(F+1)\hbar^2 \quad \text{and} \quad F_Z = m\hbar, \tag{2}$$

where $-F \leq m \leq F$

Now the magnetic moments of electrons is,

$$\mu_e = \frac{g_e \mu_B S}{\hbar}, \tag{3}$$

where μ_B is Bohr magneton its value is $9.274 \times 10^{-24}\ J/T$ and $g_e = -2.00232$.

And the magnetic moment for protons is,

$$\mu_p = \frac{g_p \mu_N I}{\hbar}, \tag{4}$$

where μ_N is Nuclear magneton its value is $5.05078 \times 10^{-23}\ J/T$ and $g_p = 5.586$.

N.B- Magnetic moment of proton is $\sim$ 650 times smaller than electrons magnetic moment.

II.b Detection of 21 cm line by Hyperfine splitting.

The interaction of energy occurs due to proton's magnetic field and electron's orbital magnetic field in the ground state is,

$$E_{\text{pot}} = -\mu \cdot \mathbf{B} \tag{5}$$

Since, Magnetic field,

$$B = \frac{\mu_0 \mu_p}{2\pi R_p^3}, \tag{6}$$

where $\mu_0 = 4\pi \times 10^7 \ TmA^{-1}$

$$E_{\text{pot}} = -\frac{4R_p^3}{3a_0^3}\mu_e B_p \tag{7}$$

Now,

$$E_{\text{pot}} = -\left(\frac{4}{3}\right)\frac{\mu_0}{2\pi}\frac{g_e g_p \mu_0 \mu_N}{a_0^3}\frac{\mathbf{S}\cdot\mathbf{I}}{\hbar^2} \tag{8}$$

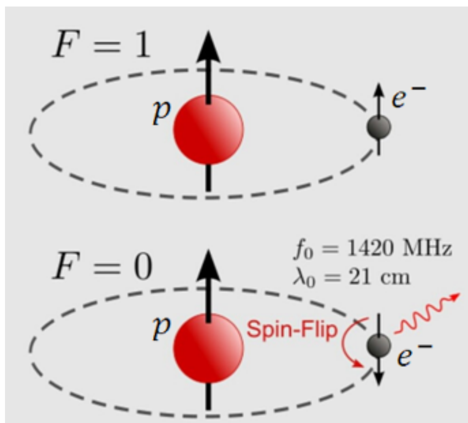

Figure 3: Hyperfine Splitting

Where

$$\mathbf{S}\cdot\mathbf{I} = \frac{\hbar^2}{2}\left[F(F+1) - S(S+1) - I(I+1)\right] \tag{9}$$

For $F = 0, S = \frac{1}{2}$ & $I = \frac{1}{2} \rightarrow \mathbf{S}\cdot\mathbf{I} = -\frac{3}{4}\hbar^2$

For $F = 1, S = \frac{1}{2}$ & $I = \frac{1}{2} \rightarrow \mathbf{S}\cdot\mathbf{I} = -\frac{1}{4}\hbar^2$

Again, For Hyperfine splitting,

We choose F =1 then,

$$E_{\text{pot}} = 1422.8 \ MHz \tag{10}$$

So, now the more precise value of the wavelength is,

$$\lambda = 21.11 \text{ cm} \tag{11}$$

III Spin Temperature

Consider the ground state of the hydrogen atom (electron in the 1s orbital and spin of the electron is anti-parallel to nuclear spin, $g_0 = 1$) and the hyper-fine excited state (1s orbital, electron spin and nuclear spin are parallel, $g_1 = 3$) i.e, the singlet and triplet state for $g_0 = 1$ and $g_1 = 3$.

The spin temperature is define as the ratio of the number of atoms in the excited state n_1 and de-excited state n_0.

$$\frac{n_0}{n_1} = \frac{g_0}{g_1} e^{-E_{10}/k_B T_s} = 3e^{-T_\star/T_s} \tag{12}$$

Where E_{10} is defined by the energy of transition from triplet to singlet state and hence corresponds to 0.068k.

Now, spin temperature can be determined by three ways:

- Spontaneous de-excitation of H-atoms from triplet to singlet state due to background CMB photons.
- Collision with other H-atoms, electrons and protons.
- Scattering due to the presence of Lyman-α photons.

IV Brightness Temperature

The Brightness temperature [1,2,13,14] of a black body is in thermal equilibrium can be determined by an optical measurement and observed at a frequency ν.The intensity at frequency ν is represented by an effective temperature called brightness temperature T_B.

The Planck's law of black body is at low frequency and high wavelength is defined as Rayleigh Jean's law for black body radiation distribution as:

$$I_\nu = B_\nu \tag{13}$$

$$B_\nu = \frac{2\nu^2 k_B T_b}{c^2} \tag{14}$$

$$\text{or,} \quad I_\nu = \frac{2\nu^2 k_B T_b}{c^2} \tag{15}$$

$$T_b = \frac{I_\nu c^2}{2\nu^2 k_B} \tag{16}$$

Where, T_b is the brightness temperature for low frequency or high wavelength, Blackbody Radiation of Spectrum, c is the velocity of light in vacuum, k_B is the Boltzmann constant.

V CMB & CMB-Temperature

The present age of the Universe is about a million years. As if we compare the history of early age to the present age we have three observables these are:

- the abundance of light elements,

- the cosmic microwave background radiation
- The dark matter.

V.a Calculation of CMB temperature:

From Planck's blackbody radiation we have the number of density of photons N_ν in the interval of frequency range ν to $\nu + d\nu$ is

$$\frac{dN_\mu}{d\nu} = \frac{8\pi\nu^2}{c^3}\frac{1}{e^{\frac{h\nu}{k_B T_0}} - 1} \tag{17}$$

Where, T_0 =temperature at the present Universe and c is the velocity of light in free space. If we consider the early age of the universe is t years , $t > t_0$, where t_0 is the current time of the Universe. Now at the early time we may predicts red shift of the photons is $(1+z) = a(t)/a(t_0)$ where a(t) is the scale factor.

The frequency ν is related to the present time t_0.Then we measure the frequency as $\nu' = \nu/(1+z)$ that implies $d\nu' = d\nu/(1+z)$.

Now the number density is, $dN_{\nu'} = dN_\nu/(1+z)^3$

From the above information we get,

$$\frac{dN_{\nu'}}{d\nu'} = \frac{dN_\nu/(1+z)^3}{d\nu/(1+z)} = \frac{1}{(1+z)^2}\frac{dN_\nu}{d\nu} \tag{18}$$

Putting equation (17) we get,

$$\frac{dN_{\nu'}}{d\nu'} = \frac{1}{(1+z)^2}\frac{8\pi\nu^2}{c^3}\frac{1}{e^{\frac{h\nu}{k_B T_0}} - 1} \tag{19}$$

Again putting $\nu = \nu'(1+z)$ we get,

$$\frac{dN_{\nu'}}{d\nu'} = \frac{1}{(1+z)^2}\frac{8\pi\nu'^2(1+z)^2}{c^3}\frac{1}{\exp\left(\frac{\frac{h\nu'}{1+z}}{k_B T_0}\right) - 1} \tag{20}$$

$$\frac{dN_{\nu'}}{d\nu'} = \frac{1}{(1+z)^2}\frac{8\pi\nu'^2(1+z)^2}{c^3}\frac{1}{\exp\left(\frac{h\nu}{k_B T(z)}\right) - 1} \tag{21}$$

Where $T_z = T_{\text{CMB}} = T_0(1+z) = T_0/a(t)$, the CMB temperature for black body radiation.

At the present age of the Universe the red shift $z = 0$ and the CMB temperature is equal to, $T_{\text{CMB}} = T_0 \approx 2.725K$

VI Optical Depth

VI.a Definition:

Optical depth is defined as the product of the material density (ρ) and the change in cross-section area of the material (ds).

$$d\tau = \alpha\rho ds \tag{22}$$

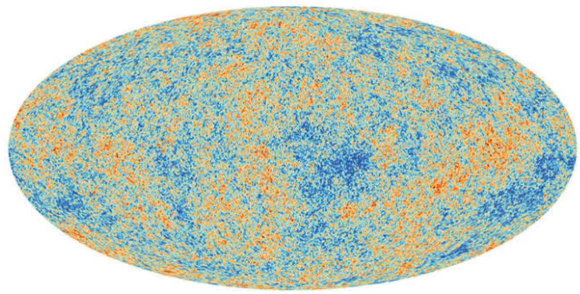

Figure 4: CMB Temperature (Image credit: Space.com)

Where α, absorption coefficient =[absorbing cross-section + scattering photons per unit mass of material](Its SI unit is m^2kg^{-1})

Now change in intensity is proportional to the intensity of the material.

$$dI = -Id\tau \tag{23}$$

$$dI = -\alpha\rho dsI \tag{24}$$

$$I = I_0e^{-\alpha\rho s} \tag{25}$$

$$I = I_0e^{-\tau} \tag{26}$$

Where, $\tau = \alpha\rho s$, optical depth is a dimensionless quantity.

From equation (26) we define optical depth as:

- When $\tau = 1$, then intensity falls by 1/e.
- When $\tau \gg 1$, optically thick.
- When $\tau \leq 1$, optically thin.

VI.b Calculation of the Optical Depth:

The optical depth is properly defined as:

$$\tau_\nu = \int_{l_0}^{l} \alpha_\nu(l')dl' \tag{27}$$

Where α_ν is the absorption coefficient [14–18] and its define as,

$$\alpha_\nu = \frac{h_p\nu_e}{4\pi}\phi(\nu)\left[n_0B_{01} - n_1B_{10}\right] \tag{28}$$

In the above equation we find the line profile function, $\phi(\nu)$, B_{01} and B_{10} are the Einstein coefficients.

We have $B_{01} = 3B_{10} = \frac{3\lambda_e^2 A_{10}}{2h_p c}$ and $A_{10} = 2.85 \times 10^{-15} s^{-1}$

And

$$\Delta\nu = \left(\frac{\partial r(\nu)}{\partial \nu}\right)^{-1} (\Delta l/a) \tag{29}$$

Since,

$$\int \phi(\nu) dl = a^2 \frac{\partial r(\nu)}{\partial \nu} \tag{30}$$

Putting the above form we get,

$$\tau_\nu = \left(\frac{h_p \nu_e}{4\pi}\right) n_0 B_{01} \left(1 - \frac{n_1 g_0}{n_0 g_1}\right) a^2 \left|\frac{\partial r(\nu)}{\partial \nu}\right| \tag{31}$$

Using $T_s > T_\star$ we get,

$$\tau_\nu = \frac{3 n_{HI} h_p c^2 A_{10} a^2}{32\pi k_B T_s \nu_e} \left|\frac{\partial r(\nu)}{\partial_\nu}\right| \tag{32}$$

Now we use

$$\frac{\partial r(\nu)}{\partial \nu} = \frac{\partial r(\nu)}{\partial a} \frac{\partial a}{\partial \nu} \tag{33}$$

Where 'a' is the scale factor comes from the Comoving distance.

As we put $\nu = a\nu_e$ and $\frac{\partial a}{\partial \nu} = 1/\nu_e$

$$\left|\frac{\partial r(\nu)}{\partial \nu}\right| = \frac{c da}{a^2 H(a) \nu_e} \tag{34}$$

And,

$$n_{HI} = \frac{\rho_{HI}}{m_H} = \frac{(\frac{\rho_{HI}}{m_H)\overline{\rho}_H}}{\overline{\rho}_H} = \frac{3\Omega_{b0}\rho_{c0}\rho_{HI}}{4 m_H \overline{\rho}_H}(1+z)^3 \tag{35}$$

, $\overline{\rho}_H = \frac{3\rho_b}{4}$, $\frac{\rho_b}{\rho_{co}} = \Omega_b = \Omega_{b0}(1+z)^3$, $\rho_{co} = 3H_0^2/8\pi G$ and the mass of the proton is $6.67 \times 10^{-27} kg$ $H_0 = 100h$ km/s/Mpc.

Finally from equation (32) we may written the optical depth as,

$$\tau = \frac{4mk}{T_s} \left(\frac{\Omega_{bo} h^2}{0.02}\right) \left(\frac{0.7}{h}\right) \left(\frac{H_0}{H(z)}\right) (1+z)^3 \left(\frac{\rho_{HI}}{\overline{\rho}_H}\right) \tag{36}$$

Where the quantity $\frac{\rho_{HI}}{\overline{\rho}_H}$ is define the ratio of the neutral hydrogen density and the mean hydrogen density [19].

VI.c Analytical Study of the optical depth:

In the fundamental idea of optical depth in 21 cm cosmological model [20–22] the plot has carried out with the Hubble constant $H(t)$ and z.

But in cosmology we know that,

$$H^2(t) = H_0^2[\Omega_r a^{-4} + \Omega_m a^{-3} + (1-\Omega) a^{-2} + \Omega_\Lambda] \tag{37}$$

Since we have 70% of Dark Energy, 26% of Dark Matter and 4% of Baryons.

So, we choose the baryonic energy density parameter $\Omega_{b0} \sim 0.04$, matter density $\Omega_m \sim 0.3$, radiation density $\Omega_r \sim 8.4 \times 10^{-5}$, Curvature density $\Omega_\Lambda \sim 0.7$ and $= 0.0$. We also assume that neutral hydrogen density is equal to the mean hydrogen density that implies $\rho_{HI} = \overline{\rho}_H$. Here we take the variation of spin temperature T_s in the following graph τ_ν Vs z, lower the value of T_s the slope is more in the graph and for more value of T_s the slope is almost flat.

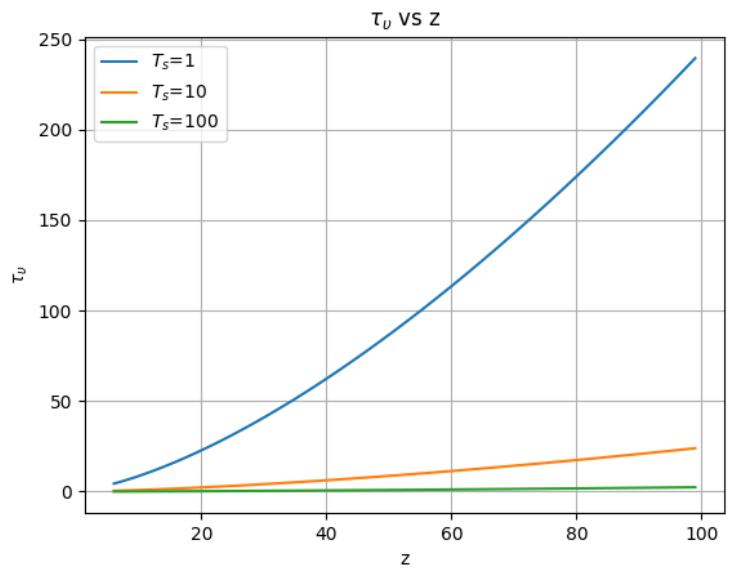

Figure 5: Optical depth (τ_ν) Vs red shift (z) for different values of spin temperature (T_s), $h = 0.7$ and $H_0 = 71$ km/sec/Mpc.

VII Specific Intensity And Differential Brightness Temperature

As we see before in project 1, the brightness temperature is coming from the approximation of Planck's law of Black body radiation at a high wavelength that is usually known as Rayleigh-Jeans law. We found the relation between specific intensity, wavelength and the brightness temperature this is $I_\nu = \frac{2k_B T\nu^2}{c^2}$, where k_B is the Boltzmann's Constant and c is the speed of light in vacuum.

VII.a Specific Intensity.

The specific intensity is defined as the area(dA) that is normal to the direction of any given ray and assume that all rays are passing through dA whose direction is within the solid angle ($d\Omega$) of the given rays and this rays only allow within a frequency interval ($d\nu$).

The specific intensity is actually defined as,

$$I(\nu) = \frac{dE}{dAdtd\Omega d\nu} \tag{38}$$

The unit of Specific intensity is in c.g.s is $ergsec^{-1}cm^{-2}str^{-1}Hz^{-1}$.

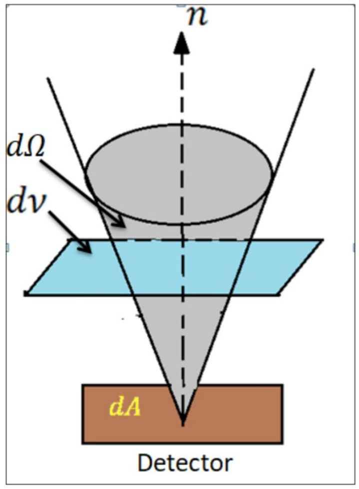

Figure 6: Specific Intensity

Now if we consider that there is in the path that depend on the coordinate, s due to radiative transfer we get,

$$\frac{dI_\nu}{ds} = -\alpha_\nu I_\nu + j_\nu \tag{39}$$

Where α_ν is absorption coefficient and j_ν is the emission coefficient.

VII.b Calculation of Differential Brightness Temperature.

From equation (39) we get the expression due to radiative transfer as

$$\frac{dI_\nu}{ds} = -\alpha_\nu I_\nu + j_\nu \tag{40}$$

$$\frac{dI_\nu}{d\tau_\nu} = -I_\nu + B_\nu(\tau_\nu) \tag{41}$$

Where τ_ν is the optical depth which is equal to $\int \alpha_\nu ds$ and B_ν is the Planck function.

Now, equation (41) may be written in terms of brightness temperature as,

$$\frac{dT_b}{d\tau_\nu} = -T_b + T_\gamma \tag{42}$$

And we find that $\delta T_b = -\frac{1}{a(t)}\left(\frac{dT_b}{d\tau_\nu}\right)$,

So, from equation (42) we get,

$$\delta T_b = (T_b - T_\gamma)a(t) \tag{43}$$

Where a(t)=1/(1+z)

For emergent radiation we finds the general expression of brightness temperature as a function of ν is,

$$T_b(\nu) = T_s\left(1 - e^{-\tau_\nu}\right) + T_\gamma e^{-\tau_\nu} \tag{44}$$

Now, from equation (43) and equation (44) we get,

$$\begin{aligned}\delta T_b &= \left[T_s\left(1-e^{-\tau_\nu}\right)+T_\gamma e^{-\tau_\nu}-T_\gamma\right]a(t)\\ &= \left[\left(T_s-T_\gamma\right)\left(1-e^{-\tau_\nu}\right)\right]a(t)\\ &= \frac{\left[\left(T_s-T_\gamma\right)\left(1-e^{-\tau_\nu}\right)\right]}{1+z}\end{aligned} \tag{45}$$

$$\delta T_b = \frac{\left(T_s-T_\gamma\right)}{1+z}\left(1-e^{-\tau_\nu}\right) \tag{46}$$

If the transition for the optical depth is significantly small at all incidental red shifts, then,

$$\delta T_b \approx \frac{\left(T_s-T_\gamma\right)}{1+z}\tau_\nu \tag{47}$$

If we put the expression of the optical depth that we found in the equation (36), then the final form of the optical depth is

$$\delta T_b \approx 27 x_{HI}\left(1+\delta_b\right)\left(\frac{\Omega_b h^2}{0.023}\right)\left(\frac{0.15}{\Omega_m h^2}\frac{1+z}{10}\right)^{\frac{1}{2}}\left(\frac{T_s-T_\gamma}{T_s}\right)\left[\frac{\partial_r v_r}{(1+z)H(z)}\right]mK \tag{48}$$

Where, $\frac{\partial v_r}{\partial r}=\partial_r v_r$ is the velocity gradient along the line of sight, δ_b =baryonic density fraction and x_{HI} = fraction of neutral hydrogen.

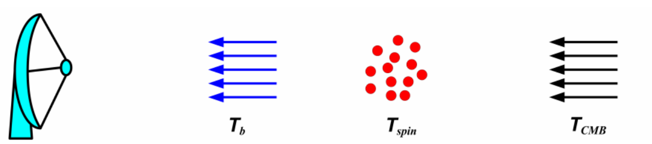

Figure 7: In the above diagram we measure the cosmological Background Temperature T_{CMB} or T_γ. Spin temperature T_S and the brightness temperature due to radiation transfer by the help of telescopes and different astronomical tools.

VII.c Analytical Study of Differential brightness temperature.

Here we plot the differential brightness temperature (δT_b) Vs red shift (z) for different values of spin temperature T_s. Here we assume that the transition for the optical depth is significantly small at all incidental red shifts so we follow the approximate value of differential brightness temperature and studied it analytically. From the plot we define that the graph is in the negative slope this implies that the value of differential brightness temperature δT_b is negative, less the value of the spin temperature T_s, magnitude of the slope is more and more the value of spin temperature T_s the slope is almost flat.

VIII Dark Matter Power Spectrum

VIII.a Dark matter power spectrum:

In our universe dark matter follows two density which are the local density and the mean density. If we see the history of the universe we like to follow the periods after reionization. As we discuss the 21 cm physics and cosmology we must follow the phase where the reionization is complete. So, we should define the dark matter power spectrum after the reionization period. The dark matter power spectrum is depends on mass density fluctuations $\Delta(z,k)$,where k is the wave number.

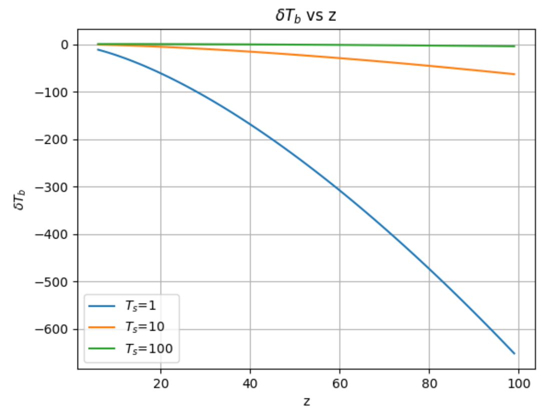

Figure 8: Differential brightness temperature (δT_b) Vs red shift (z) for different values of spin temperature(T_s), $h = 0.7$ and $H_0 = 71$ km/sec/Mpc

So, we define the power spectrum that can be written in terms of the autocorrelation function $\xi(k)$ as,

$$\xi\left(k\right) =< \Delta\left(k\right)\Delta^{\star}\left(k'\right) >= (2\pi)^3 \delta_D\left(k-k'\right)P(z,k) \tag{49}$$

where, $P\left(z,k\right)$ is the Dark matter power spectrum and $\delta_D\left(k-k'\right)$ is the Dirac delta function.

VIII.b Derivation of dark matter power spectrum:

The efficiency of 21 cm radiation is defined by $\eta_{HI}(z,n)$.

Now taking the Fourier transform of the radiation efficiency as,

$$\eta_{HI}(z,n) = \int \frac{d^3k}{(2\pi)^3} e^{-ik\cdot\widehat{n}} \eta_{HI}(z,k) \tag{50}$$

Where,

$$\eta_{HI}(z,k) = x_{HI}(z)\left(1+f\mu^2\right)\Delta(z,k) \tag{51}$$

Now, the three dimensional relevant spectra gives,

$$< \Delta(z,k)\Delta^{\star}\left(z,k'\right) > = (2\pi)^3 \delta_D\left(k-k'\right)P(z,k) \tag{52}$$

$$< \Delta_{HI}(z,k)\Delta^{\star}_{HI}\left(z,k'\right) > = (2\pi)^3 \delta_D\left(k-k'\right)P_{\Delta^2_{HI}}(z,k) \tag{53}$$

$$< \eta_{HI}(z,k)\eta^{\star}_{HI}\left(z,k'\right) > = (2\pi)^3 \delta_D\left(k-k'\right)P_{\eta^2_{HI}}(z,k) \tag{54}$$

Since P(z,k) and $P_{\Delta^2_{HI}}(z,k)$ are the power spectrum of the fluctuations in the Dark Matter and $P_{\Delta_{HI}}(z,k)$ is the cross-correlation between two power spectrum.

From equation (51) we get,

$$P_{\eta^2_{HI}}(z,k) = x^2_{HI}(z)\left(1+f\mu^2\right)^2 P(z,k) \tag{55}$$

$$= x^2_{HI}(z)\left(1+f\mu^2\right)^2 D^2(z)P_0(k) \tag{56}$$

Where, $D(z)$ is the growth factor, $P_0(k)$ is the power spectrum at the present time and f is the logarithmic derivative of the growth factor.

VIII.c Analytical Study of Dark matter power spectrum:

In the following graph we plot the dark matter power spectrum $P(k)$ Vs wave number (k) for different red shifts. We see that for the present Universe the red shift z=0, the power spectrum is more and for more red shift the power spectrum is less. So, the power spectrum is decreases with the red shift.

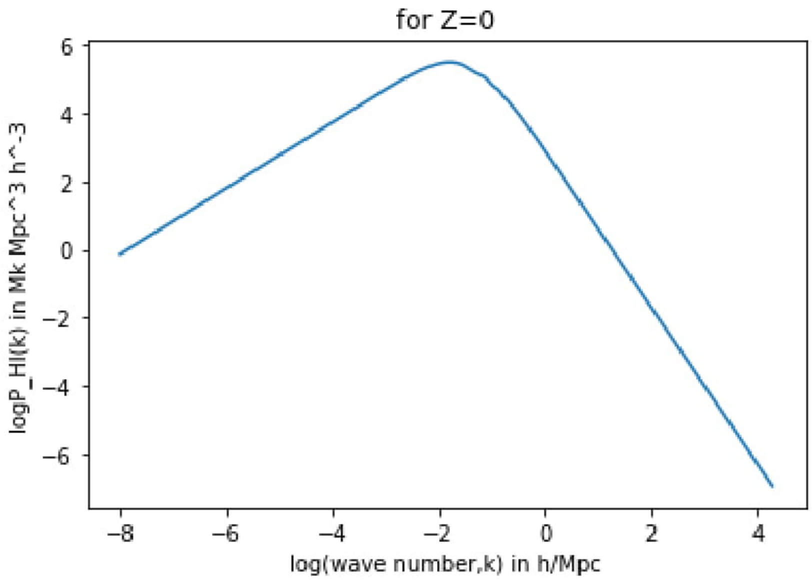

Figure 9: Dark matter power spectrum $P(k)$ Vs wave number (k) for different red shifts (z).

IX EDGES Signal & Primordial Black Hole

IX.a EDGES Signal:

The EDGES (Experiment to Detect the Global Epoch of Reionization Signature) is a radio telescope that detects the global 21 cm signal from the cosmic dawn and the epoch of reionization. The EDGES signal is an absorption profile in the frequency range 50-100 MHz, corresponding to red shifts z=6-27. The depth of the absorption profile is about 0.5 K, which is much deeper than expected from the standard cosmological model. This implies that the intergalactic medium (IGM) is much colder than expected.

IX.b Primordial Black Hole:

Primordial black holes (PBHs) are black holes that formed in the early universe due to the gravitational collapse of overdense regions. PBHs can have a wide range of masses, from the Planck mass to thousands of solar masses. PBHs can be a candidate for dark matter if they are abundant enough.

IX.c Energy injection from PBHs:

PBHs can inject energy into the IGM through accretion and Hawking radiation. The accretion of gas onto PBHs can produce X-rays and UV radiation, which can heat and ionize the IGM [23]. The Hawking radiation from PBHs can also produce photons and particles that can affect the IGM.

IX.d Constraining PBH abundance:

The EDGES signal can be used to constrain the abundance of PBHs. If PBHs are too abundant, they would inject too much energy into the IGM and prevent formation of the deep absorption profile observed by EDGES. By comparing the observed EDGES signal with theoretical models, we can put limits on the fraction of dark matter that can be in the form of PBHs.

X Conclusion

Here, we have studied the 21 cm signal from the cosmic dawn and the epoch of reionization. We have derived the expressions for the optical depth and the differential brightness temperature and studied them analytically. We have also discussed the dark-matter power spectrum and its dependence on red shift. Finally, we have explored the implications of the EDGES signal for constraining the abundance of primordial black holes. The EDGES signal suggests that the IGM is much colder than expected, which could be explained by the presence of PBHs. However, further observations and theoretical work are needed to confirm this hypothesis.

References

[1] P. J. E. Peebles. *Principles of physical cosmology*. Princeton University Press, Princeton, NJ, 1993.

[2] N. Padmanabhan and D. P. Finkbeiner. Detecting dark matter annihilation with CMB polarization: Signatures and experimental prospects. *Physical Review D*, 72(2):023508, 07 2005. arXiv:astro-ph/0503486.

[3] H. Liszt. The spin temperature of warm interstellar H I. *Astronomy & Astrophysics*, 371:698–707, 05 2001.

[4] A. Loeb and M. Zaldarriaga. Measuring the small-scale power spectrum of cosmic density fluctuations through 21cm tomography prior to the epoch of structure formation. *Physical Review Letters*, 92(21):211301, 05 2004.

[5] A. Schneider. Constraining non-cold dark matter models with the global 21-cm signal. *Physical Review D*, 98(6):063021, 2018. arXiv:1805.00021 [astro-ph.CO].

[6] H. Tashiro and N. Sugiyama. Constraints on primordial black holes by distortions of the cosmic microwave background. *Physical Review D*, 78(2):023004, 2008.

[7] S. Bharadwaj and P. S. Srikant. Radio observations of the neutral hydrogen 21 cm line from the early universe. *Journal of Astrophysics and Astronomy*, 25(1-2):67–81, 2004. In press in 2004.

[8] A. Barrau, D. Blais, G. Boudoul, and D. Polarski. Galactic cosmic rays from PBHs and primordial spectra with a scale. *Physics Letters B*, 551(3-4):218–225, 2003.

[9] F. Shankar, D. H. Weinberg, and J. Miralda-Escudé. Self-consistent models of the agn and black hole populations: Duty cycles, accretion rates, and the mean radiative efficiency. *The Astrophysical Journal*, 690(1):20–41, 2009. arXiv:0710.4488.

[10] R. Narayan and I. Yi. Advection-dominated accretion: A self-similar solution. *The Astrophysical Journal Letters*, 428:L13–L16, 1994. arXiv:astro-ph/9403052.

[11] J. Frank, A. King, and D. J. Raine. *Accretion power in astrophysics*. Cambridge University Press, Cambridge, UK, 3rd edition, 2002.

[12] C. Li and Y.-F. Cai. Searching for the dark force with 21-cm spectrum in light of EDGES. *Physical Review D*, 98(8):083536, 2018. arXiv:1805.02271 [astro-ph.CO].

[13] A. Loeb and R. Barkana. The first light. *Annual Review of Astronomy and Astrophysics*, 39:19–130, 11 2001.

[14] M. Mapelli and A. Ferrara. Background radiation from sterile neutrino decay and reionization. *Monthly Notices of the Royal Astronomical Society*, 364(1):2–12, 11 2005.

[15] A. Maselli, S. Gallerani, A. Ferrara, and T. R. Choudhury. On the size of HII regions around high-redshift quasars. *Monthly Notices of the Royal Astronomical Society*, 376(1):L34–L38, 03 2007.

[16] S. Clark, B. Dutta, Y. Gao, Y.-Z. Ma, and L. E. Strigari. 21cm limits on decaying dark matter and primordial black holes. *Physical Review D*, 98(4):043006, 2018. arXiv:1803.09390 [astro-ph.HE].

[17] T. R. Slatyer and C.-L. Wu. General treatment of the emission of strongly interacting dark matter. *Physical Review D*, 95(2):023010, 2017. arXiv:1610.06933 [astro-ph.CO].

[18] S. Bharadwaj, B. Nath, and S. K. Sethi. The first structure formation. *Journal of Astrophysics and Astronomy*, 24(1-2):23–42, 2003.

[19] C. Feng and G. Holder. Enhanced global signal of neutral hydrogen due to excess radiation at cosmic dawn. *The Astrophysical Journal Letters*, 858(2):L17, 2018. arXiv:1802.07432 [astro-ph.CO].

[20] R. Barkana and A. Loeb. Detecting the earliest galaxies through two new sources of 21cm fluctuations. *The Astrophysical Journal*, 626(1):1–11, 2005. arXiv:astro-ph/0410129.

[21] K. Lawson and A. R. Zhitnitsky. The 21cm absorption line and axion quark nugget dark matter model. *Physical Review D*, 97(12):123529, 2018. arXiv:1804.07340 [hep-ph].

[22] Jonathan R. Pritchard and Abraham Loeb. 21 cm cosmology in the 21st century. *Reports on Progress in Physics*, 75(8):086901, 2012.

[23] R. Wang, X.-B. Wu, and M.-Z. Kong. The black hole fundamental plane from a uniform sample of radio and x-ray emitting broad line AGNs. *The Astrophysical Journal*, 645(2):890–896, 2006. arXiv:astro-ph/0603514.